Field, geochemical, and isotopic evidence for magma mixing and assimilation and fractional crystallization processes in the Quottoon Igneous Complex, northwestern British Columbia and southeastern Alaska

J.B. Thomas and A.K. Sinha

Abstract: The quartz dioritic Quottoon Igneous Complex (QIC) is a major Paleogene (65–56 Ma) magmatic body in northwestern British Columbia and southeastern Alaska that was emplaced along the Coast shear zone. The QIC contains two different igneous suites that provide information about source regions and magmatic processes. Heterogeneous suite I rocks (e.g., along Steamer Passage) have a pervasive solid-state fabric, abundant mafic enclaves and late-stage dikes, metasedimentary screens, and variable color indices (25–50). The homogeneous suite II rocks (e.g., along Quottoon Inlet) have a weak fabric developed in the magmatic state (aligned feldspars, melt-filled shears) and more uniform color indices (24–34) than in suite I. Suite I rocks have Sr concentrations <750 ppm, average La_N/Yb_N = 10.4, and initial $^{87}Sr/^{86}Sr$ ratios that range from 0.70513 to 0.70717. The suite II rocks have Sr concentrations >750 ppm, average La_N/Yb_N = 23, and initial $^{87}Sr/^{86}Sr$ ratios that range from 0.70617 to 0.70686. This study suggests that the parental QIC magma (initial $^{87}Sr/^{86}Sr \approx 0.706$) can be derived by partial melting of an amphibolitic source reservoir at lower crustal conditions. Geochemical data (Rb, Sr, Ba, and La_N/Yb_N) and initial $^{87}Sr/^{86}Sr$ ratios preclude linkages between the two suites by fractional crystallization or assimilation and fractional crystallization processes. The suite I rocks are interpreted to be the result of magma mixing between the QIC parental magma and a mantle-derived magma. The suite II rocks are a result of assimilation and fractional crystallization processes.

Résumé : Le Complexe igné de Quottoon (CIQ), dioritique quartzeux, représente un corps magmatique daté du Paléogène (65–56 Ma), exposé dans le nord-ouest de la Colombie-Britannique et le sud-est de l'Alaska, et mis en place le long de la zone cisaillante du Domaine côtier. Le CIQ comprend deux suites ignées et divulgue des enseignements sur leurs régions sources et processus magmatiques. Les roches hétérogènes de la suite I (ex., le long du Passage Steamer) sont caractérisées par une fabrique intergranulaire pénétrative, de nombreux xénolites mafiques et dykes de stade magmatique terminal, des placages métasédimentaires, et des pourcentages variables de minéraux foncés (25–50). Les roches homogènes de la suite II (ex., le long du Quottoon Inlet) affichent une fabrique faiblement exprimée, développée durant le stade magmatique (feldspaths alignés, cisaillements comblés par du magma), et des pourcentages de minéraux foncés (24–34) plus uniformes que dans le cas de la suite I. Les roches de la suite I possèdent des concentrations de Sr <750 ppm, La_N/Yb_N moyen = 10,4, et des rapports $^{87}Sr/^{86}Sr$ initiaux qui varient de 0,70513 à 0,70717. Les roches de la suite II ont des concentrations de Sr >750 ppm, La_N/Yb_N moyen = 23, et des rapports $^{87}Sr/^{86}Sr$ initiaux qui varient de 0,70617 à 0,70686. Cette étude suggère que le magma parental du CIQ ($^{87}Sr/^{86}Sr$ initial $\approx$ 0,706) a pu être dérivé par fusion partielle d'un réservoir-source amphibolitique, sous les conditions similaires à celles de la croûte inférieure. Les données géochimiques (Rb, Sr, Ba, et La_N/Yb_N) et les rapports $^{87}Sr/^{86}Sr$ écartent la possibilité que les deux suites puissent être reliées entre elles par des processus de cristallisation fractionnée ou d'assimilation et cristallisation fractionnée. Les roches de la suite I sont interprétées comme étant le produit d'un mélange du magma parental du CIQ avec un magma dérivé du manteau. D'autre part, les roches de la suite II ont été formées par des processus d'assimilation et cristallisation fractionnée.

[Traduit par la Rédaction]

Received April 17, 1998. Accepted December 15, 1998.

J.B. Thomas[1] and A.K. Sinha. Petrogenesis, Isotope Geology and Tectonics Laboratory, Department of Geological Sciences, Virginia Polytechnic Institute and State University, Blacksburg, VA 24061, U.S.A.

[1] Corresponding author (e-mail: jathoma2@vt.edu).

Introduction

The Quottoon pluton is an elongate, sheet-like body of quartz diorite located in northwest British Columbia and southeast Alaska and is part of the Coast Plutonic Complex (Hutchison 1982). It is considered to be the southern terminus of the Late Cretaceous to Eocene Great Tonalite Sill (Brew and Ford 1981; Kenah 1979; Gehrels et al. 1991;

Fig. 1. (*a*) Location maps showing the distribution of suites I and II of the Quottoon Igneous Complex (QIC) along the five transects discussed in this study. (*b*) Maps of the individual transects across the QIC showing the sample numbers and locations as solid circles. Also shown are the locations where field data were collected but no sample was analyzed for geochemistry (locations without sample numbers).

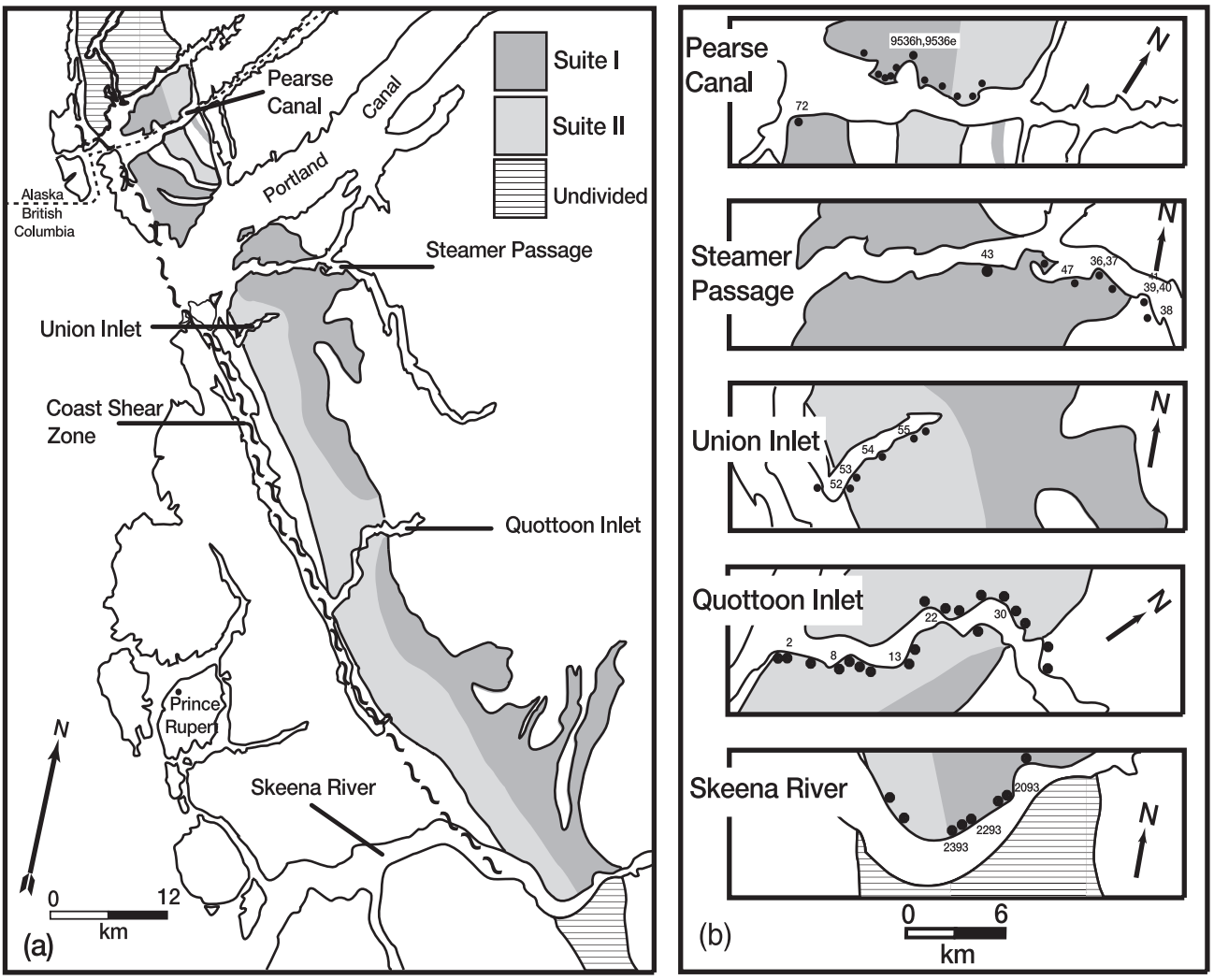

Ingram 1992). The orogen-parallel collection of plutons that make up the Great Tonalite Sill is ~1000 km long and <25 km wide. It stretches from north of Juneau, Alaska, to the headwaters of the Kowease River at 53°00′N in British Columbia (Armstrong and Runkle 1979; Kenah 1979; Hutchison 1982; Drinkwater et al. 1995 and references therein; Arth et al. 1988; Van der Heyden 1989; Gareau 1991). In northwest British Columbia and southeast Alaska, the Quottoon pluton intruded in close proximity to a major structural discontinuity, the Coast shear zone (Fig. 1*a*) (Crawford et al. 1987), which provided a zone of structural weakness for the emplacement of the Quottoon pluton and associated plutons of the Great Tonalite Sill (Brew and Ford 1981; Ingram 1992).

New field and petrographic observations, geochemical data, and Sr isotopic data from five transects across the Quottoon pluton are presented to better constrain the dominant petrologic processes responsible for its generation and subsequent magmatic evolution. Published major element geochemical data for the Quottoon pluton (Hutchison 1982) combined with recent field and geochemical evidence demonstrate the occurrence of distinct igneous suites within the Quottoon pluton (Fig. 1*a*) (Sinha et al. 1996; Thomas and Sinha 1997; Thomas 1998). A distinct structural and geochemical boundary across strike indicates that the Quottoon pluton is an igneous complex (the Quottoon Igneous Complex (QIC)) composed of physically and chemically distinct magmas emplaced in close spatial association (Fig. 1*a*).

Field relations

The QIC stretches over a distance of ~100 km from the Skeena River to Pearse Canal, and is less than 15 km wide (Fig. 1*a*). The rocks are quartz dioritic in composition and intrude the upper amphibolite facies gneisses of the Central Gneiss Complex (Hutchison 1982; Crawford et al. 1987). Most of the western contact is in close proximity to the Coast shear zone (<3 km) except near the Skeena River, at which point it is ~5 km from the Coast shear zone. Field observations along five transects from the Skeena River to

Pearse Canal (Figs. 1*a*, 1*b*) suggest that there are mappable differences in color indices, association of mafic enclaves and dikes, deformation style, and degree of wall-rock involvement along individual transects which result in definition of two distinct igneous suites.

The suite I rocks are lithologically heterogeneous, ranging from mafic quartz diorites with abundant mafic enclaves (Steamer Passage and Pearse Canal) to strongly foliated quartz diorites (Steamer Passage and eastern portions of the pluton along the Skeena River), as well as felsic quartz diorites with abundant rusty metasedimentary xenoliths and screens (portions of the pluton along the Skeena River and Pearse Canal). The origin of the mafic enclaves and dikes is uncertain, but the xenoliths and screens appear similar to the rusty metasedimentary wall rocks of the Central Gneiss Complex. Well-developed hornblende–biotite foliations, grain-size reduction, and elongate enclaves (length to width ratio >10) document the strongly deformed nature of the suite I rocks. It is likely that the observed fabric styles developed through solid-state deformation (Ingram 1992). The foliation attitude is ~240, 70 SE, and is oblique to the Coast shear zone (Fig. 1*a*).

In contrast, the suite II quartz diorites are undeformed, contain primary magmatic features, do not contain abundant metasedimentary xenoliths or screens, have equidimensional textures (e.g., plagioclase and hornblende of ~1.5 cm), and are coarser grained than rocks of suite I. Suite II rocks are located along Quottoon Inlet, Union Inlet, and the western portion of the Skeena River transect (Fig. 1*b*) and are homogeneous throughout and contain magmatic foliations (flow-aligned plagioclase and hornblende) and melt-filled shears indicative of deformation in the presence of melt (Ingram 1992). The attitude of the magmatic foliations is ~330, 80 NE, and they are parallel to the regional orientation of the Coast shear zone. The rocks along central portions of Quottoon and Union inlets are unfoliated. Mafic enclaves and late-stage dikes are present in suite II but occur in discrete zones. The absence of solid-state deformational features and the general lack of mafic enclaves provide a means for identification of suite II rocks in the field.

Mafic dikes range from 10 cm to 2 m in width, are fine grained, and have random orientations and distributions. In all cases the dikes are interpreted as late-stage features because they have sharp boundaries and fine-grained textures indicative of rapid chilling. Also, some dikes crosscut the magmatic foliations in suite II rocks, further supporting the interpretation that they represent late-stage igneous activity. The mafic dikes are especially abundant along the Steamer Passage and Pearse Canal transects. Mafic enclaves are parallel to the foliation in deformed rocks of suite I, whereas they are randomly oriented in the undeformed rocks of suite II. Also, some mafic enclaves in suite I occur only as "ghosts" as a result of extensive interaction with the host rocks, whereas other enclaves have sharp boundaries suggesting rapid chilling and limited physical interaction with the host magma (suites I and II).

Petrography

The majority of the samples from both suites I and II plot within the quartz-diorite field of Streckeisen (1973) (Table 1).

Table 1. Percent modal mineral abundances for samples from the QIC.

	Suite I										Suite II								Enclaves		Dikes	
Sample No.:	36	39	40	41	43	47	72	2093	2293	2393	536h	2	8	13	22	30	52	53	54	55	536e	37	17d	44d
Rock type:	QD	QD	QD	QD	QD	QD	QD	QD	QD	QD	QD	QD	QD	QD	QD	QD	QD	QD	QD	QD	D	D	D	D
Plagioclase	62	62	57	43	59	60	62	66	67	60	58	63	64	63	62	69	59	56	60	69	40	42	64	54
Biotite	16	28	22	16	13	21	10	17	16	12	6	11	15	23	19	19	13	15	15	10	20	19	21	17
Hornblende	13	5	14	33	17	11	18	9	11	22	31	14	12	7	12	8	20	18	17	13	38	34	10	23
K-feldspar	2	1	2	3	3	1	tr	tr	nd	tr	1	1	1	2	tr	1	nd	1	1	tr	tr	nd	tr	3
Quartz	6	4	3	5	8	6	10	8	6	6	4	10	8	4	5	2	7	9	6	7	tr	2	1	1
Apatite	tr	tr	tr	tr	tr	2	tr	tr	tr	tr.	tr	tr	tr	tr	tr	tr	tr	tr	1	tr	tr	1	1	tr
Titanite	tr	tr	tr	tr	tr	tr	tr	nd	tr	tr	tr	tr	tr	1	tr	tr	1	tr	tr	tr	tr	1	2	2
Opaques	1	tr	tr	1	1	tr	tr	tr	tr	tr	tr	tr	tr	tr	tr	tr	tr	tr	tr	1	tr	tr	1	1
Zircon	tr	tr	tr	tr	tr	tr	tr	tr	tr	tr	tr	tr	tr	tr	tr	tr	tr	tr	tr	tr	tr	tr	tr	tr
Chlorite	nd	nd	nd	nd	nd	nd	nd	tr	nd	nd	nd	tr	tr	tr	nd	nd	nd	nd	nd	nd	nd	nd	nd	nd
Epidote	tr	tr	nd	nd	nd	nd	tr	tr	nd	tr	nd	tr	1	tr	nd	tr	tr	tr	nd	tr	nd	tr	tr	nd
Sericite	tr	nd	tr	tr	tr	nd	tr	tr	nd	nd	nd	tr	tr	tr	nd	tr	nd	nd	nd	nd	nd	tr	nd	tr
hb:bi	0.8	0.2	0.6	2.1	1.3	0.5	1.8	0.5	0.7	1.9	5.3	1.3	0.8	0.3	0.6	0.4	1.6	1.2	1.2	1.3	1.9	1.8	0.5	1.4
Color index	30	34	37	50	31	34	28	25	27	34	37	28	26	31	32	27	34	34	33	24	60	56	35	43

Notes: Six hundred points were counted for each thin section. Sample 536h is the proximal host to the mafic enclave sample 536e. QD, quartz diorite; D, diorite; tr, volume of mineral <1%; nd, not detected; hb:bi, hornblende-to-biotite ratio.

Table 2. Major and trace element abundances for samples from the QIC.

	Suite I										
Sample No.:	36	39	40	41	43	47	72	2093	2293	2393	536h
SiO_2 (wt.%)	53.71	62.69	53.65	53.59	56.11	63.06	62.39	62.31	60.26	58.99	54.85
TiO_2	1.26	0.87	1.42	1.23	0.90	0.76	0.70	0.72	0.83	0.85	0.85
Al_2O_3	17.75	17.00	18.30	15.86	18.52	17.28	16.25	16.16	16.85	16.87	18.15
FeO_t	8.73	5.27	9.15	9.70	6.98	5.33	5.73	5.18	5.74	6.60	8.64
MnO	0.13	0.07	0.13	0.15	0.09	0.08	0.10	0.10	0.11	0.12	0.15
MgO	4.13	1.85	3.76	5.77	3.41	2.39	2.54	2.96	2.90	3.74	3.74
CaO	6.98	4.88	6.61	7.89	6.84	5.39	5.23	4.89	5.68	6.30	8.52
Na_2O	3.75	3.98	3.75	2.99	4.07	4.20	3.54	3.97	3.99	3.87	4.01
K_2O	2.00	1.76	2.33	1.44	1.53	1.78	2.08	2.25	1.59	1.87	1.19
P_2O_5	0.43	0.27	0.43	0.44	0.60	0.27	0.22	0.18	0.21	0.20	0.22
Total	98.87	98.64	99.53	99.06	99.05	100.54	98.78	98.72	98.16	99.41	100.32
LOI	0.67	0.35	0.5	0.55	0.51	0.34	0.37	0.65	1.55	0.80	0.41
Rb (ppm)	54	49	57	38	32	51	69	48	36	51	20
Sr	725	636	640	549	1135	687	642	649	545	608	742
Ba	1295	1120	1328	987	1096	1368	1128	na	na	na	603
Zr	235	216	148	72	138	160	90	130	109	116	253
Y	26	16	20	23	14	17	17	14	21	22	33
Hf	6	4	4	2	4	4	3	na	na	na	7
Nb	15	9	19	13	8	11	10	6	8	6	13

Notes: na, not analyzed; nd, not detected.

Table 3. Rare earth element abundances for samples from the QIC.

	Suite I										
Sample No.:	36	39	40	41	43	47	72	2093	2293	2393	536h
La (ppm)	38.2	25.9	31.6	23.7	20.3	30	19.2	22	22.2	21	20.7
Ce	73.4	48.8	61.3	49.1	41.6	52.9	40.0	44	46	44	57.3
Nd	32.5	21.1	27.6	24.4	19.7	22.3	18.9	20	20	19	35.9
Sm	6.8	4.2	5.5	5.3	4.2	4.6	4	4	4.1	4.2	8.2
Eu	1.7	1.6	1.8	1.5	1.3	1.3	1.4	1.1	1.1	1.2	1.9
Gd	5.8	5	4.8	5	3.6	3.9	4.2	na	na	na	8.1
Tb	0.8	0.6	0.6	0.7	0.5	0.5	0.6	0.4	0.5	0.5	1.1
Dy	4.5	2.8	3.6	4	2.5	3.0	2.8	na	na	na	5.7
Ho	0.9	nd	0.7	0.8	0.5	0.6	nd	na	na	na	nd
Er	2.6	1.5	2.0	2.3	1.3	1.7	1.6	na	na	na	3.2
Tm	0.33	0.2	0.3	0.3	0.2	0.2	0.2	na	na	na	0.4
Yb	2.1	1.2	1.8	2.0	1	1.4	1.5	1.2	1.9	2.1	2.7
Lu	0.34	0.2	0.3	0.3	0.2	0.2	0.2	0.2	0.3	0.3	0.4
Eu/Eu*	0.84	1.0	1.1	0.9	1.0	1.0	1.0	—	—	—	0.7
La_N/Yb_N	12.2	14.4	11.7	7.9	13.6	14.3	8.6	12.2	7.7	6.8	5.1

Notes: Abbreviations as in Table 2.

The two suites exhibit minor differences in modal abundance of alkali feldspar, which is generally more abundant in suite I. The quartz diorites of suite I have a wide range of color indices (25–50) and variable hornblende to biotite ratios (0.2–5.3) which do not correlate with geographic location or color index (Table 1). In contrast, limited variations in color indices and hornblende to biotite ratios (24–34 and 0.3–1.6, respectively) are observed in suite II (Table 1). Textural relationships indicate that both suites have similar sequences of crystallization with early crystallizing opaque minerals (magnetite and ilmenite), zircon, and titanite, followed by apatite, hornblende, biotite, and plagioclase. Quartz and potassium feldspar are the latest crystallizing phases.

Mafic dikes and enclaves from both suites plot in the diorite field of Streckeisen (1973). The mineralogy and sequence of crystallization of mafic enclaves and dikes are similar to those of the host quartz diorites except that they have higher percentages of mafic silicates (Table 1). Enclaves and dikes are fine grained (~1 mm) and have a wide range of color indices (35–60) (Table 1). The hornblende (1–5 mm) in enclaves has a well-developed sieve texture and occurs in reaction relation with clusters of greenish-brown to reddish-brown groundmass biotite, titanite, opaque oxides,

Table 2 (*concluded*).

Suite II									Enclaves		Dikes	
2	8	13	22	30	52	53	54	55	536e	37	17d	44d
60.44	58.63	59.87	62.34	60.33	60.62	58.03	58.53	56.80	50.31	47.32	48.68	50.84
0.73	0.92	0.99	0.70	0.78	0.79	0.83	1.15	0.94	1.37	1.52	1.37	1.61
17.12	16.69	17.05	16.91	17.18	17.01	18.46	16.60	18.86	17.98	19.19	20.41	20.44
5.64	6.91	6.26	5.38	5.88	5.79	5.95	7.15	6.67	10.52	11.30	10.46	8.56
0.08	0.13	0.09	0.08	0.10	0.09	0.08	0.10	0.09	0.17	0.17	0.14	0.11
2.67	3.38	2.80	2.41	2.79	3.25	2.93	3.50	3.20	4.72	5.40	3.76	3.59
5.25	5.87	5.69	5.02	5.60	5.86	6.64	6.72	6.82	8.10	8.76	8.94	7.98
3.71	3.68	4.19	4.00	4.01	3.74	4.22	3.54	4.21	3.58	3.28	4.20	4.49
2.70	1.84	1.75	2.49	1.77	1.98	1.69	1.76	1.50	2.09	2.39	1.50	1.58
0.22	0.26	0.32	0.24	0.24	0.23	0.27	0.30	0.30	0.36	0.41	0.55	0.54
98.56	98.31	99.01	99.57	98.68	99.36	99.10	99.35	99.39	99.20	99.74	100	99.74
0.51	0.61	0.43	0.35	0.56	0.36	0.42	0.60	0.39	0.45	0.76	0.35	0.57
54	45	40	64	39	42	37	37	32	59	58	23	36
911	944	1079	782	926	847	1142	931	1116	693	618	1448	1338
2245	1197	1195	1189	1191	1107	1154	1102	1146	1437	1264	940	1466
154	142	176	144	105	109	138	233	107	215	96	134	168
11	16	12	12	10	10	12	21	11	32	31	19	15
4	4	5	4	3	3	4	6	3	6	3	3	4
8	9	10	11	9	8	8	14	7	16	9	10	14

Table 3 (*concluded*).

Suite II									Enclaves		Dikes	
2	8	13	22	30	52	53	54	55	37	536e	17d	44d
22.2	47.9	26.4	36.7	25.9	28.2	53.0	25.2	33.3	19.3	25.8	22.0	23.8
40.1	91.0	53.0	64.2	45.9	51.9	86.6	60.9	57.3	43.5	66.3	51.2	53.0
17.7	33.9	23.5	23.9	18.4	19.3	27.2	31.9	21.8	24.7	39.0	28.4	26.4
3.6	6.1	4.6	4.1	3.4	3.5	4.4	6.8	3.9	6.2	8.6	6.2	5.5
1.2	1.5	1.4	1.1	1.1	1.0	1.3	2.2	1.2	1.8	2.2	1.9	1.6
3.1	4.7	3.7	3.5	3.0	3.0	3.4	5.4	3.3	5.7	8.2	5.1	4.4
0.4	0.6	0.4	0.5	0.4	0.4	0.4	0.7	0.4	0.8	1.2	0.7	0.6
2.2	3.0	2.3	2.3	1.9	1.8	2.2	3.7	2.0	5.2	5.7	3.6	2.6
0.4	0.6	0.4	0.4	0.4	0.3	0.4	0.7	0.4	0	0	0.6	0.5
1.1	1.6	1.1	1.2	1.0	1.0	1.2	1.9	1.1	3.2	3.3	1.9	1.3
0.12	0.2	0.1	0.2	0.1	0.1	0.1	0.2	0.1	0.4	0.4	0.2	0.2
0.8	1.2	0.8	1.0	0.8	0.8	1.0	1.6	0.9	2.6	2.7	1.4	1.2
0.12	0.2	0.1	0.2	0.1	0.1	0.2	0.3	0.1	0.4	0.4	0.2	0.2
1.1	0.8	1.1	0.9	1.1	0.9	1.1	1.1	1.1	0.9	0.8	1.0	1.0
18.5	26.0	22.1	24.5	21.7	23.6	35.4	10.5	24.7	5.0	6.4	10.5	13.3

and fine-grained plagioclase. These features are accentuated in the enclaves that have reacted extensively with the host quartz diorite. No refractory restitic minerals such as garnet or pyroxene are present in any of the analyzed mafic enclaves.

Whole-rock and Sr-isotope geochemistry

Analytical techniques

Fresh whole-rock samples weighing 5–20 kg were reduced in a steel-faced jaw crusher and split to ensure representative sampling. A split from each sample (~150 g) was powdered in a tungsten carbide shatterbox to <200 mesh. Major elements were measured by fusion inductively coupled plasma (ICP); trace and rare earth element (REE) abundances were measured by fusion inductively coupled plasma – mass spectroscopy (ICP–MS) at Activation Laboratories, Ancaster, Ontario, Canada. With the exception of major elements with less than 0.5 wt.% and trace elements with less than 10 ppm, both accuracy and precision are generally between 5 and 10%. The REE analyses have a reported accuracy and precision of ~10%. For Sr isotopic analyses, whole-rock samples (~50 mg) were dissolved in a HF–HNO_3 mixture using Savillex dissolution bombs at ~100°C

Table 4. Sr isotopic data for samples from the QIC.

Sample No.	$\frac{^{87}Sr}{^{86}Sr_m}$	$\frac{^{87}Sr}{^{86}Sr_i}$
Suite I		
36	0.70581(8)	0.70563
39	0.70572(2)	0.70553
40	0.70642(8)	0.70620
41	0.70622(4)	0.70605
47	0.70583(10)	0.70565
72	0.70743(7)	0.70717
2093	0.70650(11)	0.70632
2293	0.70529(5)	0.70513
2393	0.70554(8)	0.70528
536h	0.70678(7)	0.70672
Suite II		
2	0.70691(5)	0.70677
8	0.70622(10)	0.70618
13	0.706319(5)	0.70623
22	0.70706(21)	0.70686
52	0.70698(3)	0.70659
53	0.70647(11)	0.70639
54	0.70627(10)	0.70617
55	0.70638(4)	0.70631
Mafic enclaves		
37e	0.70607(8)	0.70585
536e	0.70681(7)	0.70660
Central Gneiss Complex		
893	0.70525(6)	0.70506
1293	0.70470(14)	0.70459
1593	0.70602(7)	0.70526
38	0.70610(8)	0.70530
GMO	0.70496(3)	0.70464

Notes: $^{87}Sr/^{86}Sr_m$, measured ratio; $^{87}Sr/^{86}Sr_i$, initial ratios age corrected to 58.6 Ma. Numbers in parentheses are ± two standard errors of the mean ($2\sigma_m$). Central Gneiss Complex samples: 893, felsic gneiss; 1293, metatonalite; 1593, garnet gneiss; 38, rusty metasediment; GMO, garnet sillimanite gneiss (provided by Lincoln Hollister).

for 7 days. The entire solution was centrifuged and processed to separate Sr using ion exchange techniques with a procedural blank of <150 pg. Samples were loaded onto a Re filament with Ta_2O_5, and $^{87}Sr/^{86}Sr$ ratios were determined on an automated VG-54 mass spectrometer at Virginia Polytechnic Institute and State University. $^{87}Sr/^{86}Sr$ ratios were corrected for mass fractionation using $^{86}Sr/^{88}Sr$ value of 0.1194. Replicate analyses (n = 6) of the Eimer and Amend $SrCO_3$ standard gave a value of 0.70808 ± 7 (2σ) during the course of this work.

Twenty-four samples from five transects across the QIC (see Fig. 1*b* for sample locations) were selected for major, trace, and rare earth elements and Sr isotopic analyses. Table 2 lists the major and trace element contents, Table 3 shows the REE concentrations, and Table 4 lists the initial $^{87}Sr/^{86}Sr$ ratios (Sr_i). Twenty samples are quartz diorites, two are dioritic mafic enclaves, and two are dioritic mafic dikes (Table 1). One enclave was analyzed along with its proximal host quartz diorite (samples 536e and 536h).

Suite I

The quartz dioritic rocks from suite I have a SiO_2 range from 53.6 to 63.1 wt.% (Fig. 2) that does not correlate with geographic location. All samples from suite I show large variations among all major elements at constant SiO_2 concentration, and significant variations in TiO_2, Al_2O_3, MgO, CaO, and K_2O illustrate the chemical heterogeneity of the rocks.

Large variations also exist amongst the large ion lithophile elements (LILE) and the high field strength elements (HFSE) in the suite I rocks. Rb decreases by 40 ppm between 54 and 56 wt.% SiO_2 and increases from 32 ppm to 69 ppm over a SiO_2 range of ~6 wt.% in the higher silica rocks (Fig. 2). Sr concentrations range from 549 to 742 ppm and define a shallow trend over the entire silica interval (Fig. 2), although sample 43 has a higher Sr abundance. The low-silica rocks show considerable variation in Ba (603–1328 ppm) at constant SiO_2. In mid-ocean-ridge basalt (MORB) normalized diagrams the suite I rocks have elemental abundances similar to those of the suite II rocks but are more enriched in HFSE (Fig. 3). The rocks have high LILE to HFSE ratios ($Ba_N/Y_N >> 20$) typically attributed to a subduction-related origin (Hawkesworth et al. 1994; Pearce and Peate 1995).

Suite I rocks have shallow REE patterns (average $La_N/Yb_N = 11.4$) and smooth trends that do not show significant anomalies (Fig. 4; Table 3). Only small Eu anomalies (range of Eu/Eu* = 0.8–1.1) are developed (Table 4). The REE abundances for suite I samples have a larger range and notably lower La_N/Yb_N ratios than in suite II (see below). The Sr_i ratios range from 0.70513 to 0.70717 (Fig. 5; Table 4). No simple correlation exists with silica; however, an important feature to be noted is the significant variation in Sr_i ratios (0.70553–0.70672) over a small silica range of ~1 wt.% SiO_2 in the most mafic rocks (Fig. 5). The higher-silica rocks have a range of Sr_i ratios from 0.70513 to 0.70717.

Suite II

Suite II rocks have silica concentrations ranging from 56.8 to 62.3 wt.% SiO_2 (Fig. 2) and, like the suite I rocks, show no correlations with geographic position. TiO_2, FeO_t, MgO, and CaO display negative and coherent trends with increasing silica. In contrast to other major elements, K_2O displays a strong positive and coherent correlation with increasing SiO_2. Unlike the suite I rocks, the suite II rocks do not exhibit large variations among most major elements at a given silica concentration.

Rb concentrations display a strong positive trend ranging from 32 to 64 ppm over the entire SiO_2 interval (Fig. 2). Sr concentrations range from 1142 to 782 ppm and display a coherent negative trend throughout the silica interval. Ba has a flat trend and constant concentration (relative to suite I) ranging from 1102 to 1197. Most HFSEs do not correlate well with SiO_2, but show a much narrower range in abundance at a given silica concentration than in rocks of suite I. In MORB-normalized plots (Fig. 3), the suite II rocks display a pattern similar to that of the suite I rocks but are somewhat lower in HFSE. Samples from suite II have high LILE to HFSE ratios (e.g., $Ba_N/Y_N >> 45$) that are significantly higher than those of suite I.

Fig. 2. Discrimination diagrams for representative trace elements (in ppm) from the Quottoon Igneous Complex. SiO_2 is in wt.%. The line connects an enclave host pair. ×, suite I; ●, suite II; □, mafic enclaves; △, mafic dikes.

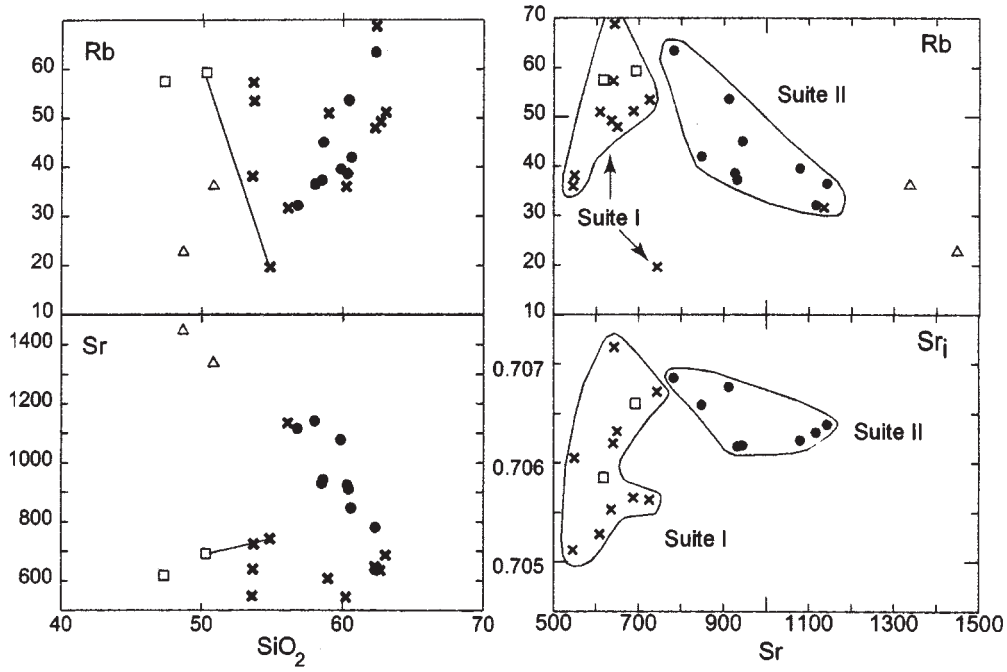

The rocks of suite II have steep REE patterns, with an average La_N/Yb_N of 23 (Fig. 4; Table 3). In comparison to suite I, the average La_N/Yb_N ratios are two times larger in suite II. Most patterns decrease smoothly and lack marked anomalies. No significant Eu anomalies are developed in suite II samples (Eu/Eu* = 0.8–1.1, Table 3). The Sr_i ratios for samples from suite II (0.70617–0.70686) show a weak positive correlation with increasing silica (Fig. 5). The higher isotopic values are from the most silica rich rocks (e.g., sample 22). The Sr_i ratios for the suite II samples are less variable than the Sr_i ratios of the suite I rocks.

Mafic enclaves and dikes

The mafic enclaves and dikes from suite I plot over regions similar to those of the silica-poor rocks of suite I (Fig. 2) but are distinctly more aluminous and slightly more calcic than the host quartz diorites. Relative to the adjacent host quartz diorite, the enclave from the enclave–host pair is enriched in TiO_2, FeO_t, MgO, K_2O, Ba, and Rb by factors of 1.5, 1.2, 1.3, 1.8, 2.4, and 3, respectively (Fig. 2). However, the enclave and the host have similar concentrations of CaO, Al_2O_3, Sr, Y, and Nb. The two mafic enclaves analyzed for Sr isotopes have Sr_i ratios of 0.70660 and 0.70585, which are similar to the host quartz diorites (Figs. 2, 5). The Sr_i ratios for the enclave–host pair are nearly identical (Fig. 5; Table 4), suggesting isotopic equilibration between the enclave magma and the host quartz diorite (e.g., Allen 1991).

The enclaves show distinct variations from the late-stage dikes in Al_2O_3, MgO, and K_2O at similar SiO_2 concentration. In MORB-normalized diagrams, the enclaves have higher K, Rb, Y, Th, and Yb than the dikes (Fig. 3). The dikes have steeper REE patterns (average La_N/Yb_N = 11.9) in comparison to the enclaves (average La_N/Yb_N = 5.68) (Fig. 4).

Summary of geochemical and Sr isotopic data from suites I and II

Although many geochemical parameters can be used to measure significant differences between suites I and II, we emphasize the Rb–Sr relationships, REE abundances, and Sr_i ratios as being diagnostic. A Rb versus Sr correlation diagram clearly discriminates between suites I and II (Fig. 2). The suite I rocks have Sr concentrations <750 ppm, whereas the suite II rocks have Sr concentrations >750 ppm. One sample from suite I (sample 43) with a high Sr concentration (1135 ppm) is interpreted to be the result of extensive interaction with abundant mafic dikes in the outcrop from which it was taken. The suite II rocks plot along a trend of increasing Rb with decreasing Sr. The enclaves are similar to the suite I rocks, whereas the mafic dikes plot at even higher Sr concentrations (>1300 ppm) than the rocks of suite II.

Rocks from suite I with the lowest Sr concentrations also have the lowest Sr_i ratios and define a positive trend of increasing Sr_i ratios from 0.70512 to 0.70672 with increasing Sr concentration over an interval of ~200 ppm Sr. In contrast, suite II rocks have higher Sr abundances and a more restricted range of Sr_i ratios.

As a whole, rocks of the QIC broadly define a trend of decreasing Sr_i ratios with increasing values of 1/Sr (Fig. 5), although three trends within suites I and II can be identified (Fig. 5). Two of these trends are developed in the suite I rocks (trends A and B), and a single dominant trend adequately defines the suite II data.

In the following discussion we utilize geochemical and Sr isotopic data to assess the roles of petrologic processes that may be responsible for the generation of different suites in the QIC. The range of most major and trace elements and Sr_i ratios for suite II rocks is more limited than in suite I compositions and therefore it is likely that suite II compositions

Fig. 3. N-MORB-normalized trace element abundance patterns (Saunders and Tarney 1984) for moderately to highly incompatible elements shown for representative samples of (*a*) suites I and II (samples 536b and 55, respectively), and (*b*) enclaves and dikes (samples 37 and 44, respectively). Symbols as in Fig. 2.

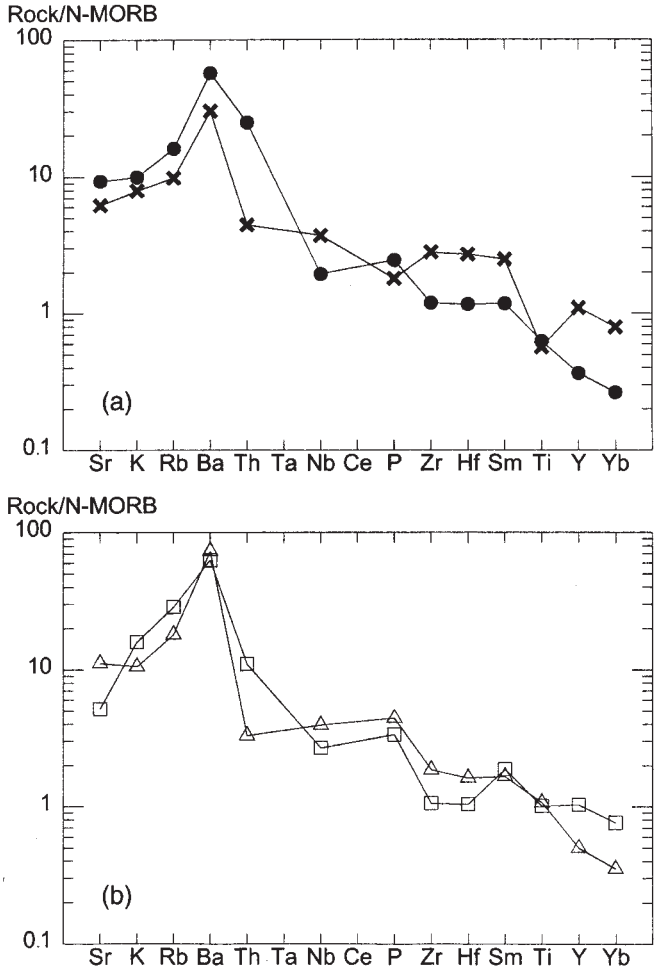

Fig. 4. Chondrite-normalized rare earth element patterns (Nakamura 1974) for (*a*) suite I, (*b*) suite II, and (*c*) enclaves and dikes. The boxed region shows the range of abundances, and the lines connect the averages in (*a*) and (*b*). Symbols as in Fig. 2.

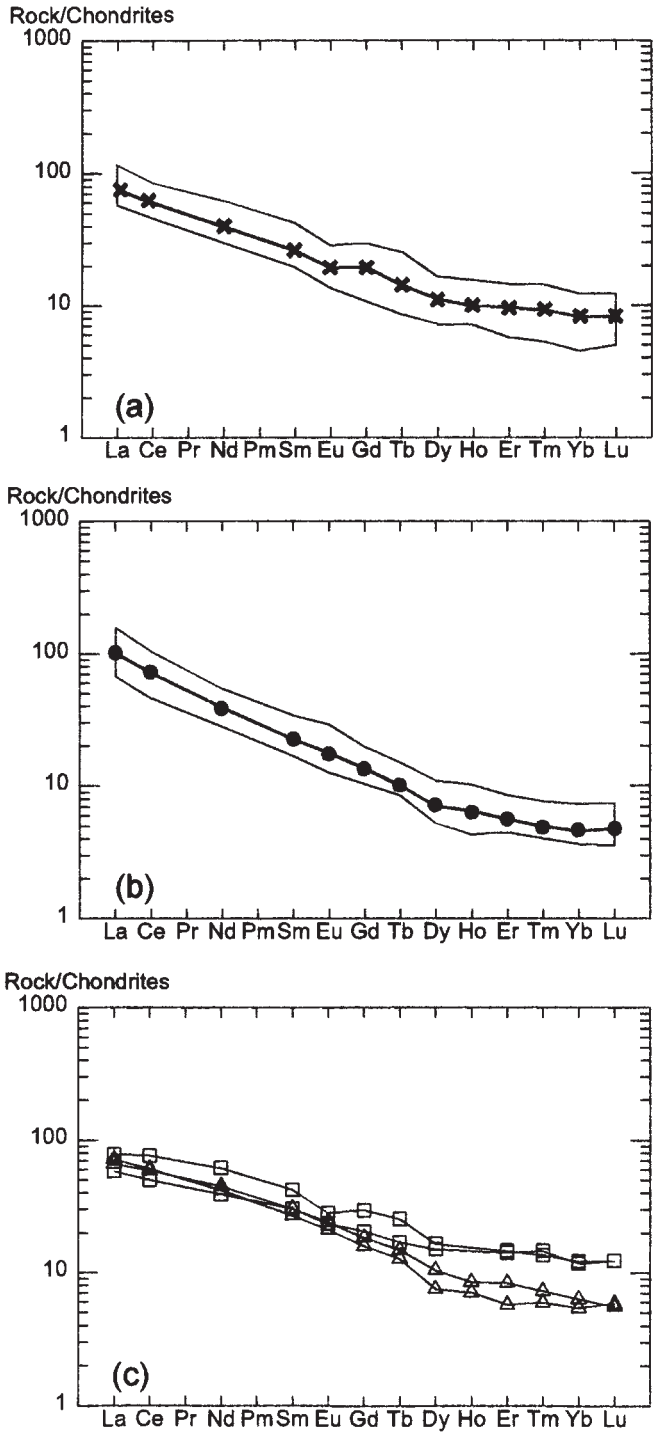

were less modified by igneous processes (e.g., magma mixing, see below) than those in suite I. Unlike the common interaction of enclaves with the host rocks of suite I, the rare mafic enclaves and dikes in suite II are fine grained, have sharp boundaries, and do not have reaction textures with the host quartz diorite, suggesting that only limited interaction and contamination by mixing may have occurred. Therefore, it is likely that the suite II rocks retain geochemical and isotopic characteristics more similar to those of the parental melts. Consequently, we utilize the rocks from suite II to constrain source region compositions and igneous processes likely to be involved in the petrogenesis of the QIC.

Petrogenesis

Source region constraints

Geochemical data and Sr_i ratios indicate that the Central Gneiss Complex is an unlikely source for the generation of the QIC. Samples from the Central Gneiss Complex analyzed for Sr isotopes yield significantly lower Sr_i ratios (0.70459–0.70530, Table 4), suggesting that the Central Gneiss Complex is not likely to be genetically related to the QIC. Available data (Hutchison 1982) combined with our new data for the Central Gneiss Complex show that the Central Gneiss Complex (where sampled) is more silica rich than the QIC. The melts generated from such bulk compositions would be more silicic than the QIC magmas. Since the

immediately adjacent Central Gneiss Complex is an unlikely protolith for melt derivation to form the QIC, other magma sources must be considered.

Experimental evidence suggests that major element abundances similar to those of the QIC suite II rocks can be generated by partial melting of amphibolites (Beard and Lofgren 1991; Rushmer 1991; Wolf and Wyllie 1994; Patiño Douce and Beard 1995). The water activity is sufficiently high in amphibolites to produce large volumes of melt (Rushmer 1991). Furthermore, the range of Sr_i ratios in many amphibolites (Sinha and Davis 1970; Samson 1990; Wendlandt et al. 1993; Borsi et al. 1995) is similar to those of the parental magma for the QIC (i.e., ~0.7063). Experimental partial melting of amphibolites demonstrates that large volumes of melt (20–50%) may form over a range of crustal pressure and temperature (*P*–*T*) conditions (3–15 kbar (1 kbar = 100 MPa) and 850–1000°C), resulting in low-potassium melts with intermediate compositions. The restite assemblages from these experiments (and their phase equilibria) provide constraints on the trace and REE composition of intermediate magmas. As demonstrated experimentally, different restite assemblages form at different pressure and temperature conditions and garnet increases in importance as a residual phase at pressures above ~10 kbar (Wolf and Wyllie 1994; Patiño Douce and Beard 1995; Winther 1996). Also, dehydration melting experiments show that plagioclase decomposes at pressures of ~14 kbar (the plagioclase-out boundary). Therefore, partial melting of an amphibolitic source reservoir at pressures >10 kbar at or near the plagioclase-out boundary (~14 kbar) could result in the elevated Sr concentrations and the heavy rare earth element (HREE) depleted nature of the QIC suite II rocks.

Modeling of batch partial melting (using eq. [11] of Shaw 1970) of an amphibolite (Table 5) is used to assess the changes in REE abundances produced by partial melting of mafic protoliths. The model uses published partition coefficients (Philpotts and Schnetzler 1970; Schnetzler and Philpotts 1970; Gill 1981). The model melts have a restite assemblage containing pyroxene (83.5–93.5%), garnet (5–15%), apatite (0.5%), titanite (0.5%), and zircon (0.5%) (Fig. 6) and are similar to those produced during experimental partial melting of amphibolites at *P* >10 kbar (Wolf and Wyllie 1994; Patiño Douce and Beard 1995). Forty percent melting produced melts that have La_N/Yb_N slopes (20.9) and Eu/Eu* (1.2) similar to those of suite II (Table 3). Because crystal fractionation of major silicate phases and (or) accessory phases only has minor influences on La_N/Yb_N, this ratio is a direct function of garnet in the restite assemblage. The QIC has slightly lower middle REE abundances than those predicted by the partial melting model. This study suggests that crystallization and removal of accessory minerals apatite and titanite from the magma after parental magma generation strongly affected the middle REE abundances.

Thus the geochemical data of the QIC coupled with the model melt compositions suggest that the parental magma composition for the QIC was most similar to that of the suite II rocks and could be generated by dehydration melting of amphibolitic compositions at pressure and temperature conditions of >10 kbar and ~1000°C. At these conditions garnet and pyroxene are stable and amphibole and plagioclase are not stable in the restite assemblage. Steep REE patterns suggest a high-pressure source (>10 kbar) where garnet was a stable residual phase, and high Sr contents (suite II average = 981 ppm, and up to 1135 ppm) imply that the source was near the plagioclase-out boundary at ~14 kbar.

Fig. 5. (*a*) Discrimination diagrams showing large variation in the suite I Sr_i ratios at constant SiO_2. (*b*) Plot of Sr_i versus 1/Sr showing two negative trends developed in suite I and a single positive linear trend in suite II. SiO_2 is in wt.% and Sr in ppm. Symbols as in Fig. 2.

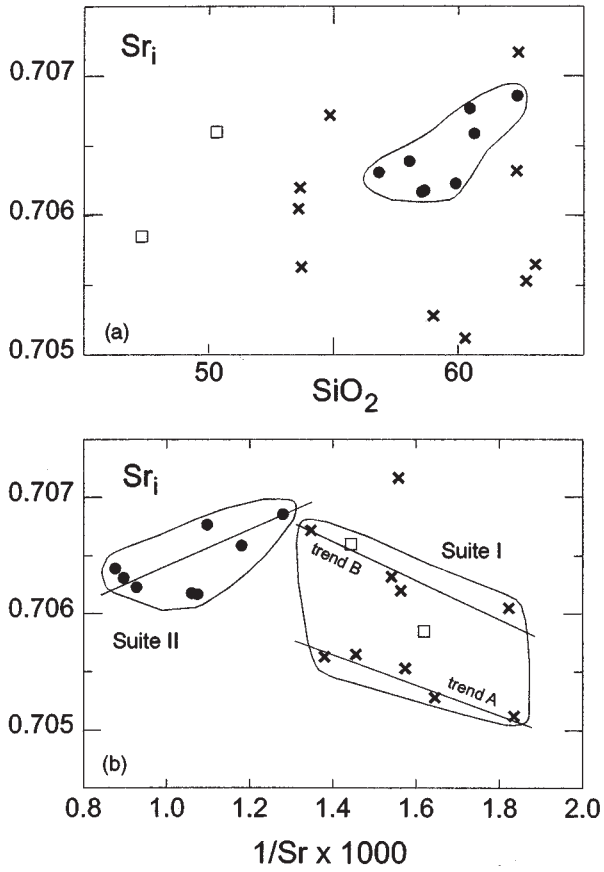

QIC evolution after parental magma generation

The range of compositions observed for the suite II rocks are best modeled by processes involving fractional crystallization. We performed least squares calculations utilizing the program and equations from Mason (1987) to assess the role of fractional crystallization. Mineral data from Kenah (1979) and Thomas (1998) were used in the calculations. Sample 55 was selected as a parental composition because (*i*) it is similar in major element composition to experimentally produced melts from amphibolites (Rushmer 1991; Wolf and Wyllie 1994), (*ii*) it has a low silica concentration that may be parental to more felsic compositions, and (*iii*) it has high Sr concentrations and low Rb concentrations that may be parental to more evolved compositions. Although the low R^2 values from the calculations (0.03) (see Defant and Nielsen 1990 for assessment of R^2 values) suggest that fractional crystallization is a likely process that could produce the range of measured geochemical compositions of suite II, the observed variability in Sr_i ratios precludes this as the sole process.

Table 5. Trace element and REE abundances (in ppm) and Sr_i of the amphibolite used for partial melting, the assimilant concentrations used in the AFC modeling, and the basalt used in magma mixing calculations.

	Rb	Sr	La	Ce	Nd	Sm	Eu	Gd	Tb	Dy	Ho	Er	Tm	Yb	Lu	$\frac{^{87}Sr}{^{86}Sr_i}$
Amphibolite	32.1	376	16.1	36.3	22.3	6.5	2.4	7.2	1.3	7.7	1.6	4.7	0.6	4.2	0.7	0.70631
E5/11	4.6	297	1.37	3.7	3.1	1.1	1.1	1.5	0.3	1.8	0.4	1.3	0.2	1.2	0.2	0.70305
Assimilant	110	650	30	64	26	4.5	0.9	3.8	2.2	3.5	0.8	2.3	0.3	2.2	0.3	0.70900

Notes: The amphibolite is from the Gravina belt of southeast Alaska. E5/11 is an island-arc basalt from New Britain (Johnson and Chappell 1979). The assimilant is a crustal composite (Taylor and McLennan 1981). Sr_i ratios for the assimilant and the amphibolite are model values.

Fig. 6. REE modeling of partial melting of an amphibolite (Table 5) with a restite assemblage containing variable amounts of garnet (gt) and clinopyroxene (cpx) (see text for details). The boxed field is the range of REE abundances from suite II. +, model compositions.

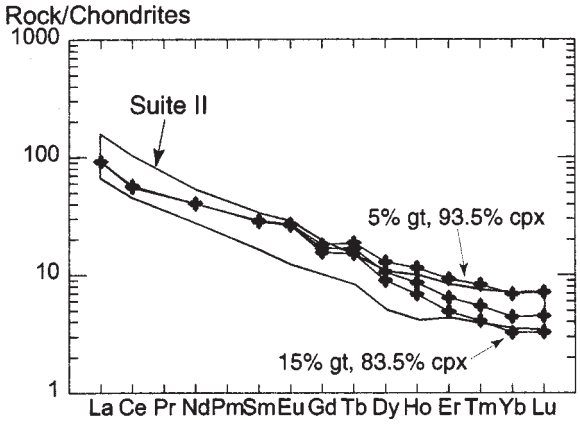

In an attempt to reconcile the Sr_i ratios and geochemical data, suite II rocks were modeled utilizing assimilation and fractional crystallization processes (AFC) (eq. [6a] of DePaolo 1981) using the same parental composition as above (sample 55). The assimilant has a fixed composition that is similar to that of average continental crust (Table 5) (Taylor and McLennan 1981). Results of the calculations obtained through removal of an assemblage containing 65% plagioclase, 34% hornblende, 0.3% titanite, 0.5% apatite, and 0.2% zircon using published partition coefficients (Philpotts and Schnetzler 1970; Schnetzler and Philpotts 1970; Drake and Weill 1975; Green and Pearson 1985; Fujimaki 1986) are shown in Figs. 7 and 8. Forty percent fractionation of the above assemblage with concurrent assimilation (ratio of assimilation rate to the fractionation rate $r = 0.3$) provides a reasonable explanation for the correlations developed in suite II between SiO_2, Rb, Sr, the REE, and Sr_i ratios. Model melt compositions produced from amphibolite partial melting (described earlier) have higher chondrite-normalized values for the middle REE than those measured for the suite II rocks (Fig. 6). AFC processes that remove apatite, titanite, and zircon from the liquid would result in REE patterns and abundances similar to those of the suite II rocks (Fig. 8). The samples that do not fit the AFC model well (Figs. 7*a*, 7*b*) may be explained through (*i*) a changing bulk distribution coefficient during crystallization (Ragland 1989), (*ii*) two separate parental magmas within suite II, (*iii*) differing rates of assimilation ($r = 1$–4) during

Fig. 7. Plots of (*a*) Rb versus Sr, and (*b*) Sr_i versus Sr. Both diagrams show the compositional trends (as shaded regions) generated by assimilation and fractional crystallization processes. The parental composition is sample 55 from suite II, and the model assimilant (✳) is a crustal composite (Taylor and McClennan 1981). The Sr_i for the assimilant is a model value. Symbols as in Fig. 2.

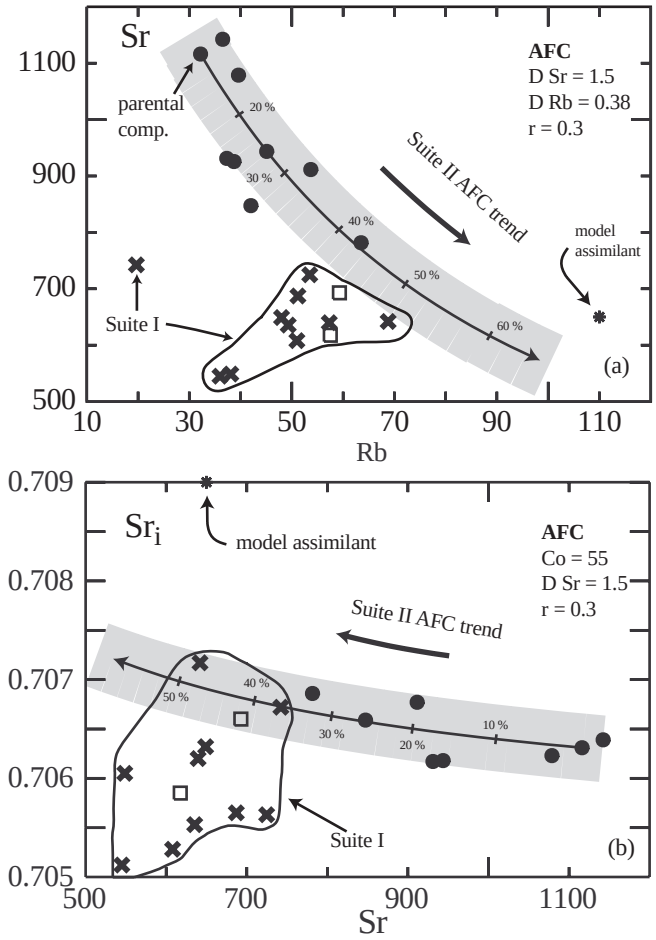

crystallization, and (or) (*iv*) various assimilants during emplacement.

At the level of emplacement, there is no field evidence for extensive assimilation in the form of abundant and reacted xenolithic material in the QIC. Furthermore, the wall rocks of the QIC consistently yield relatively low values of Sr_i ratios (0.70459–0.70530; see Table 4) and therefore did not contribute to the isotopically evolved nature of the QIC as a radiogenic assimilant. Therefore, it is likely that assimilation

Fig. 8. REE modeling of AFC processes (10–50% fractionation) for 65% plagioclase + 34% hornblende + 0.3% titanite + 0.5% apatite + 0.2% zircon removal from the model melt composition produced from the partial melting model shown in Fig. 6 (10% garnet restite). The boxed field is the range of REE abundances from suite II. +, calculated model compositions.

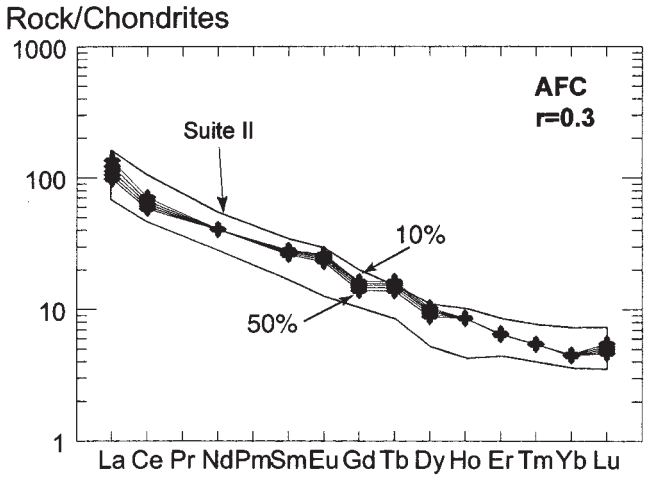

of radiogenic lithologies that affected suite II must have occurred below the level of emplacement.

The more heterogeneous rocks of suite I cannot be modeled through fractional crystallization or AFC processes. In addition to high R^2 values (>0.1) for least squares calculations, the Rb–Sr relations and a large range in Sr_i ratios suggest that fractional crystallization is not the dominant igneous process that produced the observed variations in suite I. The suite I rocks do not lie along any fractional crystallization or AFC trends but instead occur as clusters of data that have a trend opposite to that expected from fractional crystallization (Figs. 7*a*, 7*b*) (i.e., decreasing Sr with increasing Rb and Sr_i ratios for AFC processes).

The abundance of mafic enclaves in various stages of disaggregation and reaction in suite I suggests that the magma chemistry may have been affected by magma mixing processes (Vernon 1983; Frost and Mahood 1987; Allen 1991; Blundy and Sparks 1992; Holden et al. 1991). Magma mixing equations (eqs. [1]–[4] of Langmuir et al. 1978) were used to assess magma mixing processes, as well as the proportions of quartz diorite and the mafic end-member components involved in the mixing process. We assume that the mafic magma involved in mixing is basaltic in composition due to the general trend of the Sr_i ratios towards mantle isotopic compositions. The mantle end-member composition used in the model (Table 5) is an island-arc basalt from the New Britain arc (Johnson and Chappell 1979). The mafic enclaves were not chosen as the mantle end member because they have interacted and equilibrated to varying degrees with the host quartz diorites; therefore, they have inherited physical, geochemical, and isotopic characteristics from the host.

Suite I rocks do not define a single mixing line in Sr_i versus 1/Sr, but rather the data define two trends (trends A and B, Figs. 5*b* and 9). However, no simple mixing line exists that includes all of the data. Compositions along trend A can be produced through a mixture containing <65% mantle end member mixed into the QIC parental composition (i.e., sample 55 of suite II). A mixture containing <45% mantle end member mixed with sample 536h of suite I can produce the compositions along trend B. Sample 72 is isotopically the most evolved rock from suite I and may be the result of greater amounts of fractional crystallization and assimilation than the remainder of suite I. The absence of a single mixing line could have been produced through accumulation, fractional crystallization, or AFC processes where the hybrid magmas continued evolution after mixing. In this case the original magmas formed a single mixing line which underwent subsequent modification due to continued magmatic evolution through AFC processes (see Myers and Sinha 1984; Frost and Mahood 1987; Myers and Frost 1994). AFC processes would generate a trend of increasing Sr_i ratios with increasing 1/Sr (Fig. 9). Just as likely, the felsic end member may have changed composition due to fractionation processes prior to magma mixing, so the felsic end member continually fractionated throughout the mixing interval. It is not possible to discriminate between these environments. Regardless of the sequence of mixing events that affected suite I, it is clear that the data define an envelope of combined processes dominated by magma mixing with minor fractionation processes.

Fig. 9. Diagram showing a dynamic model of magmatic evolution for the QIC. The suite I rocks may have originally formed a single mixing line with the mafic end member prior to subsequent evolution through fractionation processes or the mafic end member may have mixed with a felsic end member that was undergoing AFC processes during magma mixing. The mafic end member is an island-arc basalt from New Britain (+, sample E5/11 from Johnson and Chappell 1979; see our Table 5). See text for details. The shaded regions outline the trends generated by both AFC and magma-mixing processes. Symbols as in Fig. 2.

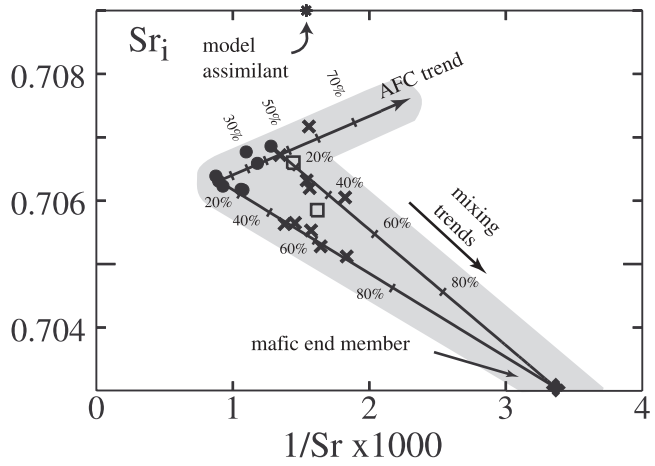

Conclusions

Differences in field, petrographic, geochemical, and isotopic data from the quartz dioritic Quottoon Igneous Complex show that it consists of two suites. The suites are physically distinct. Suite I is pervasively deformed and contains abundant mafic dikes and enclaves. The enclaves are elongate and parallel the well-developed foliation. Interaction with

the mafic enclaves modified the quartz dioritic magmas and resulted in the heterogeneous nature of suite I rocks. Geochemical and isotopic data indicate that the dominant petrologic process that operated in suite I was magma mixing in which a mantle-derived basaltic magma extensively modified a more felsic magma derived from partial melting of amphibolitic lithologies. The suite I rocks do not define a simple mixing line between the mafic magma and the more quartz dioritic end member as expected for a two-component mixture. Deviations from a single mixing line are attributed to continued evolution after magma mixing through fractionation or AFC processes. Alternatively, the end members may have continually evolved throughout the magma mixing processes.

The suite II rocks do not contain abundant mafic enclaves or dikes. The rocks are undeformed and preserve primary magmatic textures such as flow-aligned crystals and melt-filled shears. Geochemical and Sr isotopic evidence shows that AFC-dominated processes produced the observed geochemical variation within suite II. Fractional crystallization of plagioclase, hornblende, titanite, apatite, and zircon with concurrent assimilation of a more isotopically evolved lithology adequately explain the data. The AFC trends developed in suite II are discontinuous with the trends of the more mafic suite I rocks, indicating that the two suites are unrelated through any reasonable fractional crystallization scenarios. Utilizing the least evolved composition, we suggest that the parental magmas were generated by partial melting of amphibolitic lithologies at lower crustal pressure and temperature conditions.

Acknowledgments

This work was supported by the National Science Foundation (EAR-9526613) as part of the ACCRETE project. We thank M.L. Crawford, W.A. Crawford, and R. Matthews for guiding us in the field and for considerable insightful discussions. We also appreciate the countless discussions with J.S. Beard regarding all aspects of granitoid petrogenesis. We are grateful to D.B. Clarke, P. Giampiero, and an anonymous reviewer for their helpful comments.

References

Allen, C.M. 1991. Petrogenesis of the reversely zoned Turtle pluton, southeastern California. Ph.D. thesis, Virginia Polytechnic Institute and State University, Blacksburg, Va.

Armstrong, R.L., and Runkle, D. 1979. Rb–Sr geochronometry of Ecstall, Kitkiatka, and Quottoon plutons and their country rocks, Prince Rupert region, Coast Plutonic Complex, British Columbia. Canadian Journal of Earth Sciences, **16**: 387–399.

Arth, J.G., Barker, F., and Stern, T.W. 1988. Coast batholith and Taku plutons near Ketchikan, Alaska: petrography, geochronology, geochemistry, and isotopic character. American Journal of Science, **288A**: 461–489.

Beard, J.S., and, Lofgren, G.E. 1991. Dehydration-melting and water-saturated melting of basaltic and andesitic greenstones and amphibolites at 1, 3, and 6.9 kb. Journal of Petrology, **32**: 365–401.

Blundy, J.D., and Sparks, R.S.J. 1992. Petrogenesis of mafic inclusions of the Adamello massif, Italy. Journal of Petrology, **33**: 1039–1104.

Borsi, L., Petrini, R., Talarico, F., and Palmeri, R. 1995. Geochemistry and Sr–Nd isotopes of amphibolite dykes from northern Victorialand, Antarctica. Lithos, **35**: 245–259.

Brew, D.A., and Ford, A.B. 1981. The Coast plutonic complex sill, southeastern Alaska. *In* The U.S. Geological Survey in Alaska — accomplishments during 1980. *Edited by* N.R.D. Albert and T.L. Hudson. U.S. Geological Survey, Circular 823-B, pp. B99–B102.

Crawford, M.L., Hollister, L.S., and Woodsworth, G.J. 1987. Crustal deformation and regional metamorphism across a terrane boundary, Coast Plutonic Complex, British Columbia. Tectonics, **6**: 343–361.

Defant, M.J., and Nielsen, R.L. 1990. Interpretation of open system petrogenetic processes: phase equilibria constraints on magma evolution. Geochimica et Cosmochimica Acta, **54**: 87–102.

DePaolo, D.J. 1981. Trace element and isotopic effects of combined wallrock assimilation and fractional crystallization. Earth and Planetary Science Letters, **53**: 189–202.

Drake, M.J., and Weill, D.F. 1975. Partitioning of Sr, Ba, Ca, Y, Eu^{2+}, Eu^{3+} and other REE between plagioclase feldspar and magmatic liquid: an experimental study. Geochimica et Cosmochimica Acta, **39**: 689–712.

Drinkwater, J.L., Brew, D.A., and Ford, A.B. 1995. Geology, petrography, and geochemistry of granitic rocks from the Coast Mountains Complex near Juneau, southeastern Alaska. U.S. Geological Survey, Open-file Report 95-638.

Frost, T.P., and Mahood, G.A. 1987. Field, chemical, and physical constraints on mafic–felsic magma interaction in the Lamarck Granodiorite, Sierra Nevada, California. Geological Society of America Bulletin, **99**: 272–291.

Fujimaki, H. 1986. Partition coefficients of Hf, Zr, and REE between zircon, apatite and liquid. Contributions to Mineralogy and Petrology, **94**: 42–45.

Gareau, S.A. 1991. Geology of the Scotia-Qual metamorphic belt, Coast Plutonic Complex, British Columbia. Ph.D. thesis, Carleton University, Ottawa, Ont.

Gehrels, G.E., McClelland, W.C., Samson, S.D., Patchett, P.J., and Brew, D.A. 1991. U–Pb geochronology of Late Cretaceous and early Tertiary plutons in the northern Coast Mountains batholith. Canadian Journal of Earth Sciences, **28**: 899–911.

Gill, J.B. 1981. Orogenic andesites and plate tectonics. Springer Verlag, Berlin, Germany.

Green, T.H., and Pearson, N.J. 1985. Experimental determination of REE partition coefficients between amphibole and basaltic liquids at high pressure. Geochimica et Cosmochimica Acta, **49**: 1465–1468.

Hawkesworth, C.J., Gallagher, K., Hergt, J.M., and McDermott, F. 1994. Destructive plate magmatism: geochemistry and melt generation. Lithos, **33**: 169–188.

Holden, P., Halliday, A.N., Stephens, W.E., and Heney, P.J. 1991. Chemical and isotopic evidence for major mass transfer between mafic enclaves and felsic magma. Chemical Geology, **92**: 135–152.

Hutchison, W.W. 1982. Geology of the Prince Rupert – Skeena map area, British Columbia. Geological Survey of Canada, Memoir 394.

Ingram, G.M. 1992. Deformation, emplacement and tectonic inferences: the Great Tonalite Sill, southeastern Alaska, U.S.A. Ph.D. thesis, University of Durham, Durham, England.

Johnson, R.W., and Chappell, B.W. 1979. Chemical analyses of rocks from the late Cenozoic volcanoes of north-central New Britain and the Witu Islands, Papua, New Guinea. The Bureau

of Mineral Resources of Australia, Report 209, BMR Microform MF76.

Kenah, C. 1979. Mechanisms and physical conditions of emplacement of the Quottoon pluton, British Columbia. Ph.D. thesis, Princeton University, Princeton, N.J.

Langmuir, C.H., Vocke, R.D., and Hart, S.R. 1978. A general mixing equation with application to Icelandic basalts. Earth and Planetary Science Letters, **37**: 380–392.

Mason, D.R. 1987. Mix-n-Mac: a petrological least-squares mixing program. Glenside, Australia.

Myers, J.D., and Frost, C.D. 1994. A petrologic reinvestigation of the Adak volcanic center, central Aleutian arc, Alaska. Journal of Volcanology and Geothermal Research, **60**: 109–146.

Myers, J.D., and Sinha, A.K. 1984. Assimilation of crustal material by basaltic magma: strontium isotopic and trace element data from the Edgecumbe volcanic field, SE Alaska. Journal of Petrology, **25**: 1–26.

Nakamura, N. 1974. Determination of REE, Fe, Mg, Na, and K in carbonaceous and ordinary chondrites. Geochimica et Cosmochimica Acta, **38**: 757–775.

Patiño Douce, A.E., and Beard, J.S. 1995. Dehydration-melting of biotite gneiss and quartz amphibolite from 3 to 15 kb. Journal of Petrology, **36**: 707–738.

Pearce, J.A., and Peate, D.W. 1995. Tectonic implications of the composition of volcanic arc magmas. Annual Review of Earth and Planetary Sciences, **23**: 251–285.

Philpotts, J.A., and Schnetzler, C.C. 1970. Phenocryst-matrix partition coefficients for K, Rb, Sr and Ba with applications to anorthosite and basalt genesis. Geochimica et Cosmochimica Acta, **34**: 307–322.

Ragland, P.C. 1989. Basic analytical petrology. Oxford University Press, Inc., New York, N.Y.

Rushmer, T. 1991. Partial melting of two amphibolites: contrasting experimental results under fluid absent conditions. Contributions to Mineralogy and Petrology, **107**: 41–59.

Samson, S.D. 1990. Neodymium and strontium isotopic characterization of the Wrangellia, Alexander, Stikine, Taku and Yukon crystalline terranes of the Canadian Cordillera. Ph.D. thesis, University of Arizona, Tucson.

Saunders, A.D., and Tarney, J. 1984. Geochemical characteristics of basaltic volcanism within back-arc basins. *In* Marginal basin geology. *Edited by* B.P. Kokelaar and M.F. Howells. Geological Society Special Publication (London), no. 16, pp. 59–76.

Schnetzler, C.C., and Philpotts, J.A. 1970. Partition coefficients for rare earth elements between igneous matrix materials and rock forming mineral phenocrysts-II. Geochimica et Cosmochimica Acta, **34**: 331–340.

Shaw, D.M. 1970. Trace element fractionation during anatexis. Geochimica et Cosmochimica Acta, **34**: 237–243.

Sinha, A.K., and Davis, G.L. 1970. Geochemistry of the Franciscan volcanic and sedimentary rocks from California. Year Book, Carnegie Institution of Washington, **69**: 394–397.

Sinha, A.K., Thomas, J.B., Crawford, M.L., and Beard, J.S. 1996. The nature of Paleogene magmatism along the ACCRETE corridor. American Geophysical Union Fall Meeting, Abstracts with Programs, **77**:.. F652.

Streckeisen, A.L. 1973. Plutonic rocks. Geotimes, **18**: 26–30.

Taylor, S.R., and McLennan, S.M. 1981. The composition and evolution of the continental crust: rare earth element evidence from sedimentary rocks. Philosophical Transactions of the Royal Society, **A301**: 381–399.

Thomas, J.B. 1998. The petrologic significance of multiple magmas in the Quottoon Igneous Complex, northwestern British Columbia and southeastern Alaska. M.Sc. thesis, Virginia Polytechnic Institute and State University, Blacksburg, Va.

Thomas, J.B., and Sinha, A.K. 1997. The Quottoon Igneous Complex: a record of tectonic evolution along the Coast Shear Zone. Geological Society of America, Abstracts with Programs, **29**: A83.

Van der Heyden, P. 1989. U–Pb and K–Ar geochronometry of the Coast Plutonic Complex, 53°N to 54°N, British Columbia, and implications for the Insular–Intermontane boundary. Ph.D. thesis, University of British Columbia, Vancouver, B.C..

Vernon, R.H. 1983. Restites, xenoliths and microgranitoids enclaves in granites. Journal and Proceedings of the Royal Society of New South Wales, **116**: 77–103.

Wendlandt, E., DePaolo, D.J., and Baldridge, W.S. 1993. Nd and Sr chronostratigraphy of the Colorado Plateau lithosphere: implications for magmatic and tectonic underplating of the continental crust. Earth and Planetary Science Letters, **116**: 23–43.

Winther, K.T. 1996. An experimentally based model for the origin of tonalitic to trondhjemitic melts. Chemical Geology, **127**: 43–59.

Wolf, M.B., and Wyllie, P.J. 1994. Dehydration melting of amphibolite at 10 kb: the effects of temperature and time. Contributions to Mineralogy and Petrology, **115**: 369–383.